DYNAMIC CHARACTERIZATION OF A MULTI-COMPONENT FORCE TRANSDUCER USING A LORENTZ FORCE LOAD CHANGER

Jan Schleichert[1], Matthias Carlstedt[2], Rafael Marangoni[3], Ilko Rahneberg[1], Thomas Fröhlich[1]

1 Institute for Process Measurement and Sensor Technology, Department of Mechanical Engineering, Technische Universität Ilmenau, D-98684 Ilmenau, Germany

2 Department of Advanced Electromagnetics, Department of Electrical Engineering and Information Technology, Technische Universität Ilmenau, D-98684 Ilmenau, Germany

3 Department of Precision Engineering, Department of Mechanical Engineering, Technische Universität Ilmenau, D-98684 Ilmenau, Germany

ABSTRACT

Strain gauge based force transducers are often used in applications that require the measurement of static or quasi-static forces. For these measurements a static calibration is sufficient. In dynamic measurements however, the measurement deviation caused by using static calibration coefficients increases when approaching the resonance frequency of the sensor. This paper deals with the dynamic characterization of a multi-component force sensor used in Lorentz force eddy current testing, a measurement principle that is based on the measurement of dynamic force reactions. For the dynamic calibration a system is presented that allows the use of various test signals to determine the system parameters of the force transducer. Measurement results for different test signals are shown and main sources of error are discussed. Based on the estimated parameters, an inverse filter [1] can be designed to calculate the dynamic force from the measured output voltages of the sensor.

1. INTRODUCTION

New applications for accurate force measurement are arising for example in robotics [2], flow measurement [3] or nondestructive testing. Lorentz force eddy current testing (LET) is a novel non-destructive testing technique introduced in [4-6] which is based on measuring the Lorentz force acting on a system of permanent magnets during the relative motion of an electrically conductive non-ferromagnetic object under test. Due to the relative motion, eddy currents are induced inside the specimen governed by Ohm's law for moving conductors. These eddy currents are accompanied with a Lorentz force acting on the conductor, and on the magnet system itself due to Newton's 3rd law. This force is proportional to the specimens conductivity and by that an indicator for material anomalies and defects inside the specimen. In these applications the direction of the force-vector as well as its magnitude are unknown and time-dependent. Multi-component force transducers are widely used for measuring all three components of force, but are calibrated with static loads in most cases. When the measured forces are getting closer to the sensors resonance frequency, the measurement error is increasing when static calibration factors are applied. A dynamic calibration reveals the frequency response of the measurement system and is the basis for designing an appropriate filter that compensates these deviations. The dynamic investigation of single-component force transducers by using a harmonic excitation created by a shaker is known from [7]. In [8] the

measurement of the impulse response is used to identify the dynamic characteristics. For multi-component transducers a dynamic characterization was only done in [9] using a shaker and a mass to create harmonic excitation by inertial forces. In the following paper a three component force sensor model is identified using different types of force signals. These are the chirp signal, sinusoidal signal and noise signal that are applied by a voice-coil actuator as described in [10].

2. MEASUREMENT SETUP

To perform a dynamic measurement of the given multi-component force sensor, excitation-forces of up to 400 Hz were applied using a voice-coil actuator. For a complete characterization of the three-axis sensor, at least three independent measurements are required, with the actuator being aligned with each one of the three measurement axes. The force sensor is mounted in a fixed position while the voice-coil actuator is mounted in three different orientations as can be seen from Figure 1. During every measurement the responses of all measurement axes are captured which allows the determination of the main responses and the crosstalk to other components.

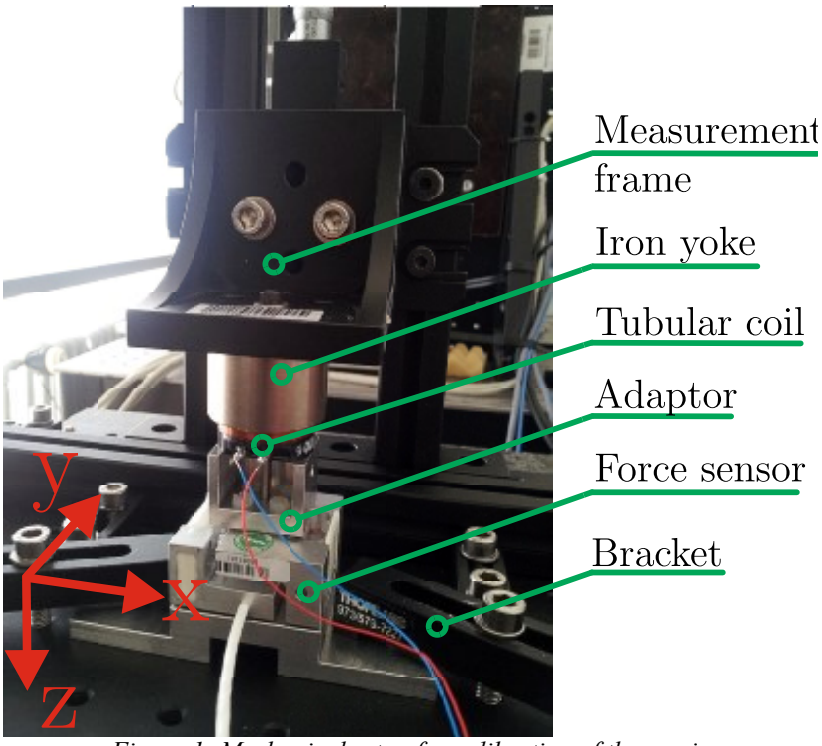

Figure 1: Mechanical setup for calibration of the z-axis

The actuator generates a Lorentz force proportional to the current, applied by a U/I-converter which translates the test signals created by a dSPACE digital signal processing unit [11]. The current through the coil is measured to calculate the acting force from the calibration constant of the actuator. The U/I Converter has a constant transfer behavior of 76.73 mA/V up to a frequency of 10 kHz with a standard uncertainty of 0.44 mA/V. A schematic of the measurement setup is shown in Figure 2. Additional to creating the test signals and measuring the coil current, the dSPACE unit is used for simultaneous sampling of the output signals of the three channels of the force sensor. The dSPACE unit is controlled by a computer, which is responsible for processing the measured data and receiving the measuring parameters, such as the measuring time and type of test signal from the user.

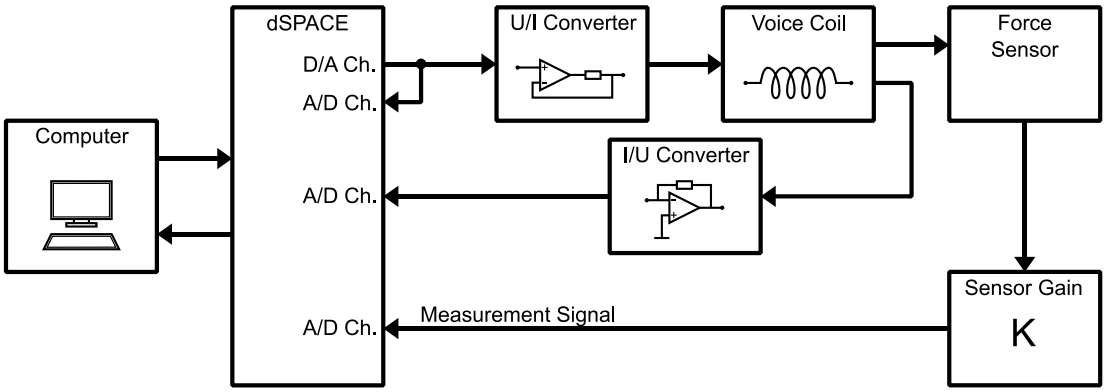

Figure 2: Electrical setup

2.1 Calibration of the Actuator

Additional to the linear dependency of the force on the current, the force depends on the position of the coil inside the magnetic field. As the coil cannot be aligned perfectly in the center position and is displaced by the acting forces because of the compliance of the force sensor under test, the assumption of a constant force sensitivity of the actuator leads to an error in calibration. To determine the force sensitivity as a function of the coil position a calibration is necessary. This is done by replacing the force sensor in Figure 1 by a calibrated EFC balance as described in [12] and changing the position of the coil with a two-axis linear stage to measure the force at different positions in the magnetic field. From this calibration of the actuator, the force sensitivity (Figure 3) was determined.

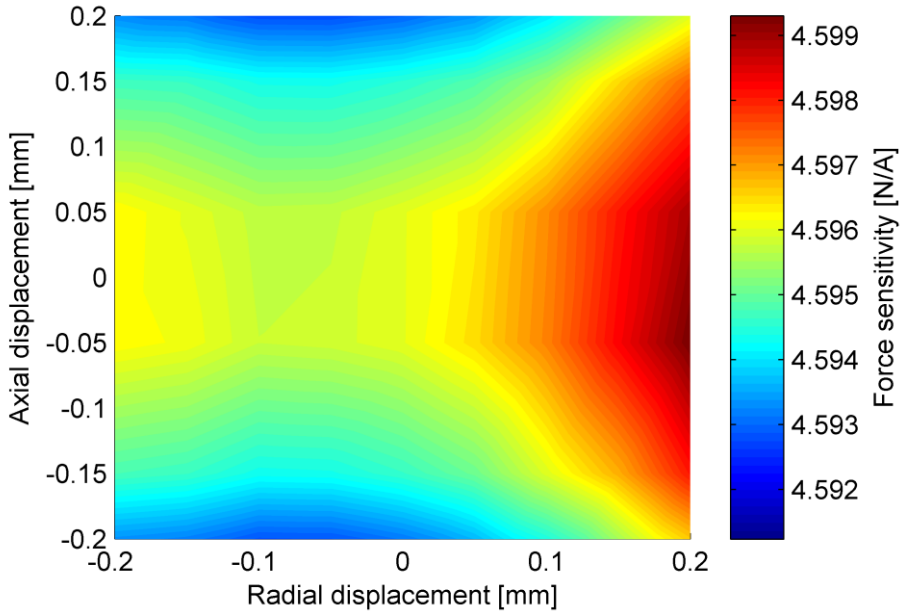

Figure 3: Force sensitivity of the voice coil actuator as a function of the axial and radial displacements

From the calibration the force sensitivity is determined to be 4.5967 N/A at the center position with a standard uncertainty of 98 µN/A. The deviation of the actuator's force caused by deviations of the coil from its center position is 4.7 mN/A in maximum. This corresponds to a relative error in applied force of 0.1 %.

2.2 Static measurement uncertainties

From the calibration of the actuator, the calibration force can be approximated by Equation 1

$$F = i_{coil} \cdot (Bl_0 + Bl_1 \cdot x^2 - Bl_2 \cdot y^2) \quad (1)$$

The coil can be aligned to a radial position x and axial position y in the range of ±0.1 mm from the centered position. The displacement from this initial position caused by the calibration force of ±0.1 N and the sensor's stiffness of about 30 N/mm [13] is estimated to be in the range of ±3 µm and was neglected in the calculation of static measurement uncertainty. In the dynamic case, this uncertainty contribution is not negligible anymore, because the amplitude of the dynamical excited motion is higher near resonance frequency. The standard uncertainty of the calibration current from the U/I converter was determined by measurement to be ±132 µA. The uncertainty budget for the measurements of the force components in x and y direction is given in Table 1. The uncertainty contribution caused by the position of the coil was estimated for maximum misalignment of 0.1 mm to avoid sensitivity coefficients of zero due to the reference value being zero as well.

Table 1: Measurement uncertainty budget

Quantity	Reference value	Standard uncertainty	Uncertainty contribution
$\mathbf{i_{coil}}$	$22.887 \cdot 10^{-3}$ A	$132 \cdot 10^{-6}$ A	$6.06 \cdot 10^{-4}$ N
x	0 m	$5.77 \cdot 10^{-5}$ m	$9.56 \cdot 10^{-15}$ N
y	0 m	$5.77 \cdot 10^{-5}$ m	$3.37 \cdot 10^{-14}$ N
$\mathbf{Bl_0}$	$4.5967 \cdot 10^{-3}$ N/A	$98 \cdot 10^{-6}$ N/A	$2.25 \cdot 10^{-6}$ N
$\mathbf{Bl_1}$	$41.78 \cdot 10^{-6}$ N/Am^2	$10.76 \cdot 10^{-6}$ N/Am^2	$9.56 \cdot 10^{-15}$ N
$\mathbf{Bl_2}$	$73.54 \cdot 10^{-6}$ N/Am^2	$3.74 \cdot 10^{-6}$ N/Am^2	$8.56 \cdot 10^{-16}$ N
Calibration force			0.1052 N
Expanded uncertainty (k=2)			$12.13 \cdot 10^{-4}$ N

2.3 Estimation of error by eddy current damping

Due to the movement of the actuators coil in the magnetic field, eddy currents proportional to the velocity are induced which counteract the acting force. The additional eddy current damping coefficient c_d can be estimated by Equation 2 from the electrical conductivity of the copper wires of the coil σ, the magnetic flux density of the permanent magnet B, the internal and external diameters of the coil d_e, d_i and the height of the coil in the field h.

$$c_d = \sigma \cdot B^2 \cdot (d_e - d_i)^2 \cdot h \cdot \frac{\pi}{4} \approx 0.2915 \ \frac{Ns}{m} \quad (2)$$

From the datasheet of the sensor [13] the values of the stiffness k and natural frequency ω_0 are approximately 30 N/mm and 220 Hz for the x and y axis. With the damping coefficient from (3) the change in damping ratio is given by

$$\Delta\xi = \frac{c_d \ \omega_0}{2 \cdot k} \approx 0.0011 \quad (3)$$

For the z-axis the stiffness with 100 N/mm and a natural frequency of 400 Hz are given in [13], which gives an estimate of $5.8 \cdot 10^{-4}$.

3. DYNAMIC CHARACTERIZATION

3.1 Methodology

Two signal analysis techniques are used for the system identification: the Orthogonal Correlation [14] and the Fast Fourier Transform. In order to apply both methods to the identification of the force sensor, it is necessary to set up a measuring system, which is capable of generating test signals, sampling external signals and processing the measured data. The test signal is a specific input which is applied to the system under test during the identification. In this work four types of test signals are considered: the sine function, the pseudo white noise, the chirp signal and the maximum length binary sequence (MLBS) signal. The measuring system is shown in Figure 2 where a dSPACE digital signal processing unit is used for generating the test signal through a D/A converter and for sampling external signals through A/D converters. The dSPACE unit is controlled by a computer, which is responsible for receiving the measuring parameters from the user, such as the measuring time and type of test signal, and for processing the measured data.

3.2 System identification through Orthogonal Correlation

In the method of Orthogonal Correlation the system under study is excited by a sine-shaped test signal and its steady state output is analyzed. With the cross-correlation function calculated between the system's input $u(t)$ and output $y(t)$

$$\phi_{uy}(\tau) = \lim_{T\to\infty} \frac{1}{T} \int_0^T u(t-\tau)y(t)\,\mathrm{d}t\,, \tag{4}$$

the system's gain $K(\omega_0)$ and phase delay $\varphi(\omega_0)$ can be determined [14]:

$$K(\omega_0) = \frac{2}{u_0^2}\sqrt{\phi_{uy}(0)^2 + \phi_{uy}(T_0/4)^2}$$

$$\varphi(\omega_0) = \arg(\phi_{\mathrm{uy}}(0) + \mathrm{j}\phi_{\mathrm{uy}}(\mathrm{T}_0/4))$$

where ω_0, T_0 and u_0 are respectively the frequency, period and amplitude of the test signal $u(t)$. By this means, equation (4) is evaluated only for $\tau = 0$ and $T_0/4$. Furthermore, its integral is calculated for a limited number $n \in \mathbb{N}^*$ of oscillation periods:

$$\phi_{uy}(\tau) = \frac{1}{nT_0} \int_0^{nT_0} u(t-\tau)y(t)\,\mathrm{d}t$$

The system's frequency response diagram can be determined by the execution of this process for different values of ω_0.

3.3 System identification through Fast Fourier Transform

The Fast Fourier Transform is a numeric efficient method for the evaluation of a signal's Discrete Fourier Transform. The computation of the Fourier Transform of a system's input signal $u(t)$ and output signal $y(t)$ provides the following relationships:

$$\mathcal{F}\{u(t)\} = U(\mathrm{j}\omega); \quad \mathcal{F}\{y(t)\} = Y(\mathrm{j}\omega)$$

Under the assumption that the system is linear, its frequency response can be determined as [15]:

$$G(\mathrm{j}\omega) = \frac{Y(\mathrm{j}\omega)}{U(\mathrm{j}\omega)}$$

By the FFT, a discrete estimative for the system's frequency response can be obtained:

$$\hat{G}(\mathrm{j}\omega_i) = \frac{\hat{Y}(\mathrm{j}\omega_i)}{\hat{U}(\mathrm{j}\omega_i)}$$

where $\hat{Y}(\mathrm{j}\omega_i)$ and $\hat{U}(\mathrm{j}\omega_i)$ are respectively the FFT of the system's input and output signal and $i \in \{x \in \mathbb{N}^* : x \leq k\}$, with $k \in \mathbb{N}^*$ equal to the domain size of the discrete frequency response function. The system's gain $K(\omega_i)$ and phase delay $\varphi(\omega_i)$ are calculated through the following expressions:

$$K(\omega_i) = \left|\hat{G}(\mathrm{j}\omega_i)\right|; \quad \varphi(\omega_i) = \arg(\hat{G}(\mathrm{j}\omega_i))$$

The input signal $u(t)$ should contain every frequency component that is relevant for the analysis. In this work three types of input signal were considered: the pseudo white noise, the chirp signal and the MLBS signal.

3.3.1 Pseudo white noise

The pseudo white noise (Figure 4) contains a series of computer generated pseudo random numbers uniformly distributed between -1 and $+1$. With this signal different frequency components can be excited at the same time.

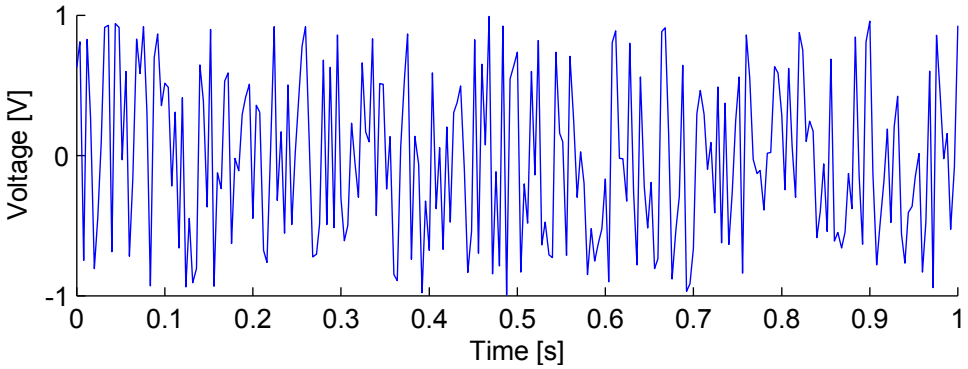

Figure 4: Pseudo white noise

3.3.2 Chirp signal

The chirp signal (Figure 5) comprises a sine function with time-dependent frequency. This signal is given by the following function:

$$u(t) = \sin\left(2\pi\left(\frac{f_1 - f_0}{2f_1}t^2 + f_0 t\right)\right)$$

where f_0 and f_1 are the initial and final frequencies respectively. On mechanical systems with resonance, the chirp signal must be carefully applied in order to avoid excessive excitation of the system at its resonance frequency.

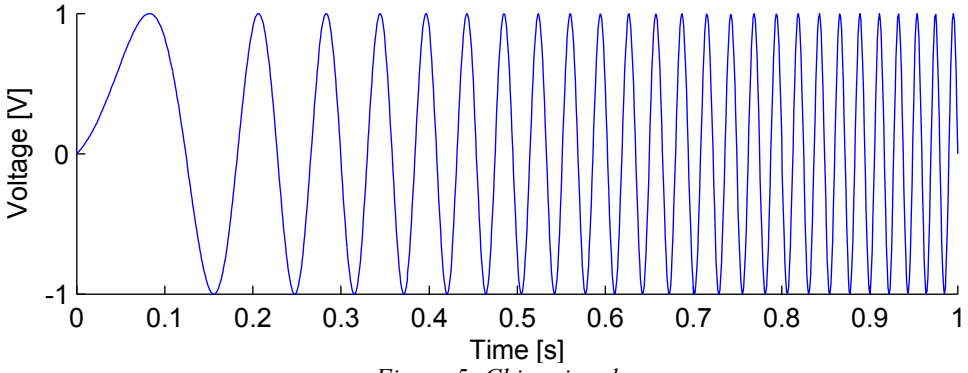

Figure 5: Chirp signal

3.3.3 MLBS signal

The MLBS signal (Figure 6, [14]) is a pseudo random, time-discrete, binary signal. Like the pseudo-random white noise, this signal is capable to excite different frequency components simultaneously.

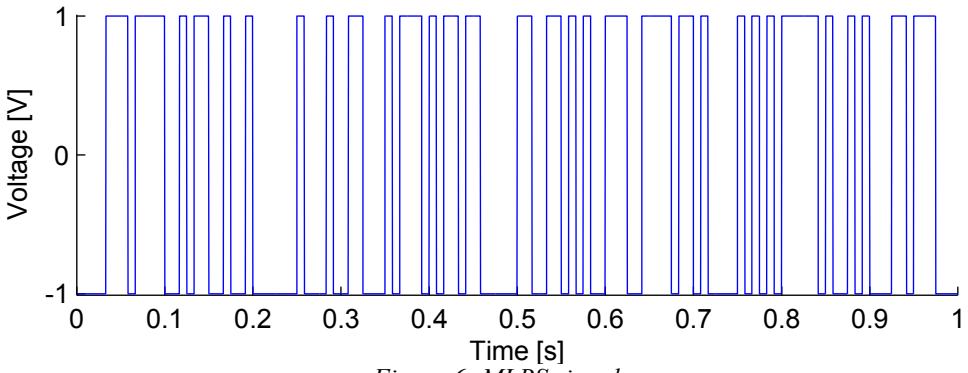

Figure 6: MLBS signal

4. SYSTEM IDENTIFICATION

The measurement setup was used to identify the dynamic behavior of the force sensor in its three directions (X, Y and Z axis). The three axes were excited seperately by means of the voice coil, using the four different test signals and the strain of the deflection elements in respective directions was measured. Figures 8, 9, 10 and 11 show the measurement results for the Z axis using the white noise, the MLBS signal, the sine function (orthogonal correlation) and the chirp signal respectively. Each measurement was executed 20 times (for orthogonal correlation 5 times), and its mean values and standard deviations are shown in the figures. The measured frequency response has a similar behavior for the four test signals, and the main difference between the plots resides in their standard deviations. The measurement with the pseudo white noise has the biggest uncertainties, followed by the results obtained through the MLBS signal. Meanwhile, the sine function and the chirp signal provided the lowest standard deviations. Since the identification through the chirp signal yields a “continuous” frequency response diagram, it has an additional advantage against the sine function.

4.1 Characterization of the Amplifier

To identify the sensor behavior separately from the measurement amplifier, its response was measured using the Chirp-signal described above (Figure 7). The amplifier has a gain of 60 dB up to a corner frequency of 1.5 kHz.

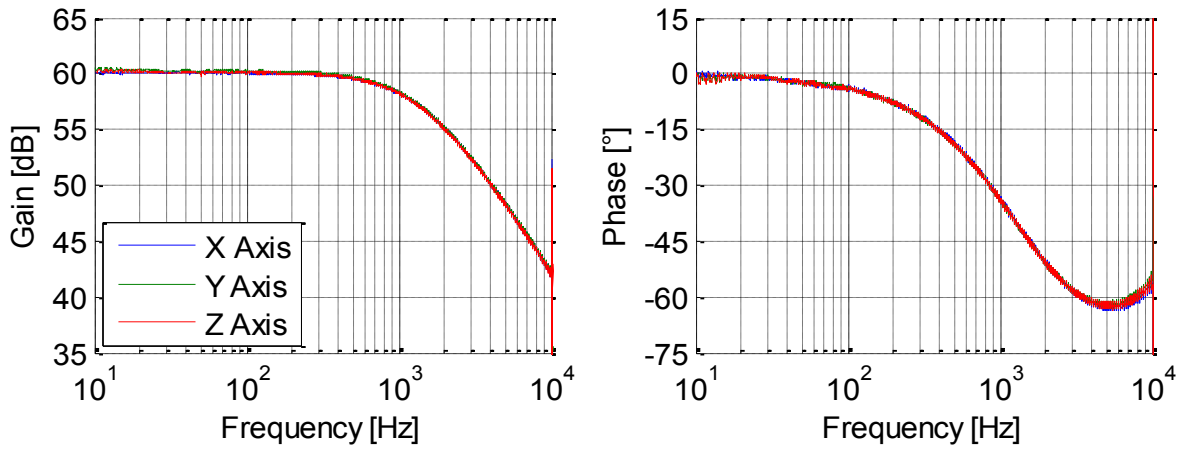

Figure 7: Frequency response diagram for the measurement amplifier

To reduce the influence of the amplifier on the measurement of the sensor-response, the sensor characterization will be done up to a frequency limit of 400 Hz.

4.2 Characterization of the Force sensor

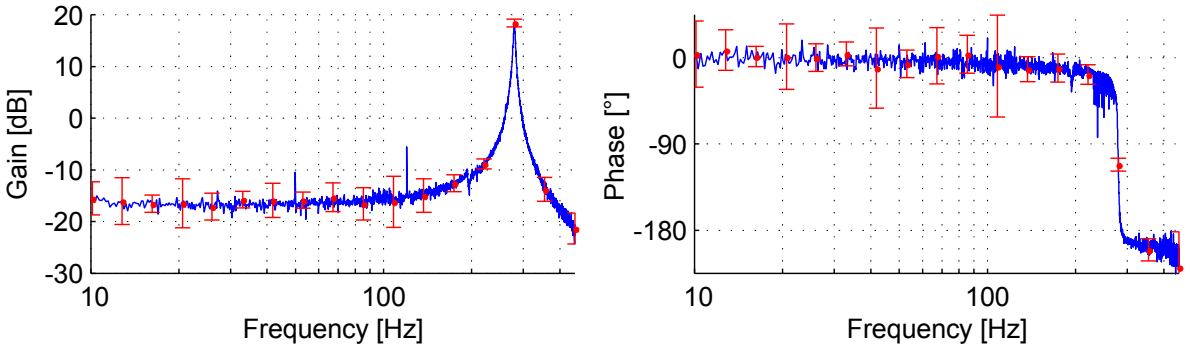

Figure 8: Frequency response for Z axis using the white noise signal

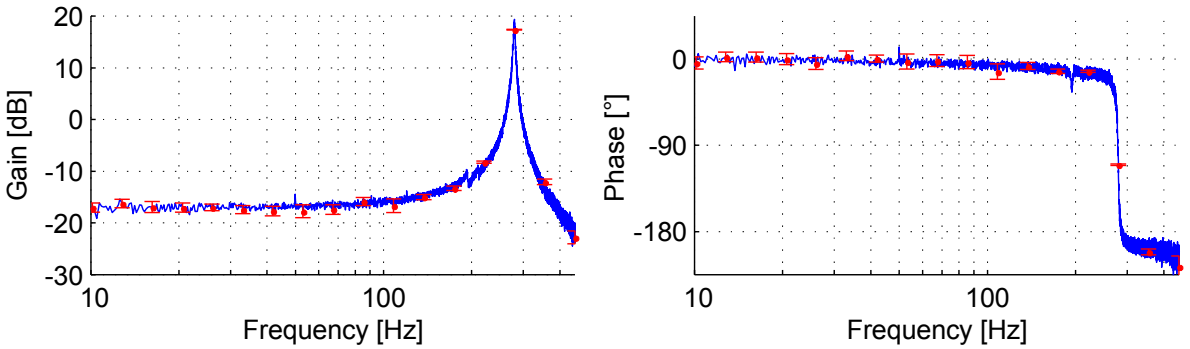

Figure 9: Frequency response for Z axis using the MLBS signal

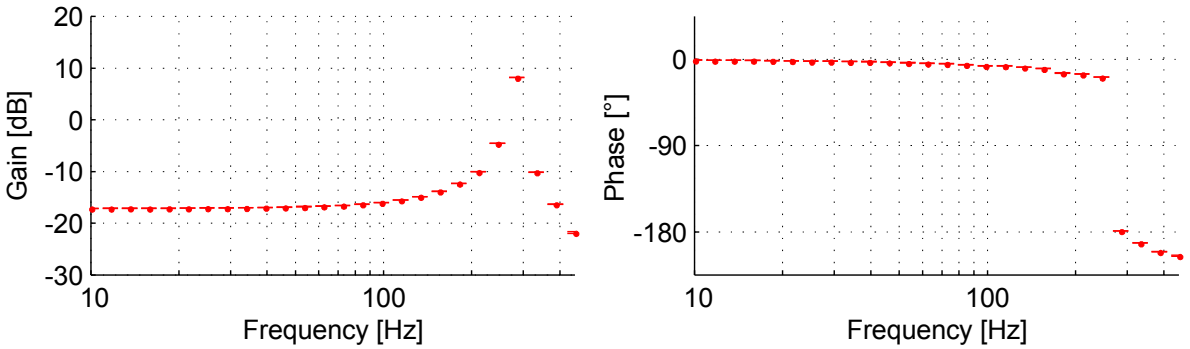

Figure 10: Frequency response for Z axis using the sinusoidal signal

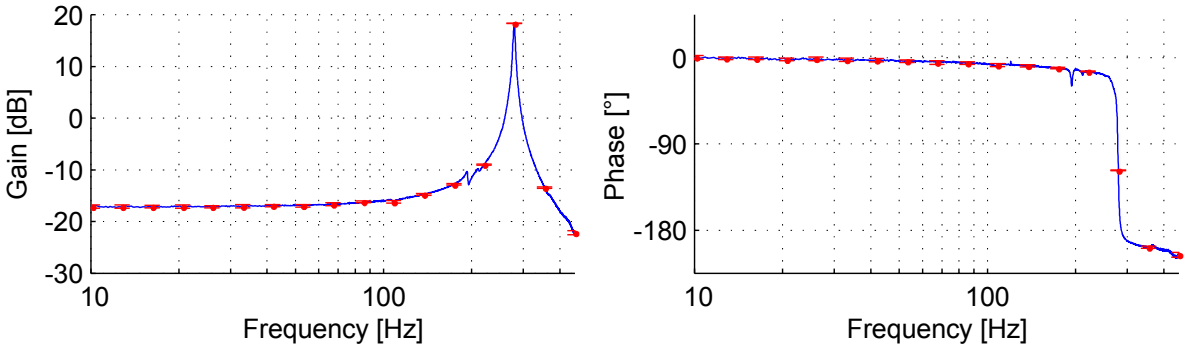

Figure 11: Frequency response for Z axis using the chirp signal

4.3 Parametric identification of the force sensor

Figure 12 contains the measured frequency response diagram for the three axis of the force sensor. All axes were measured using the chirp signal, and the plotted curves comprise the mean values of 20 measurements. These results are very similar to the frequency response of the second order transfer function

$$G(s) = \frac{K\omega_0^2}{s^2 + 2\xi\omega_0 s + \omega_0^2},$$

with $K, \omega_0 \in \mathbb{R}^+$ and $\xi \in \{x \in \mathbb{R} : 0 < x < 1\}$. Through the parametric optimization of the error function

$$e(K, \omega_0, \xi) = \int_{\omega_1}^{\omega_2} (|G(\omega \mathrm{j})| - G_M(\omega))^2 \, \mathrm{d}\omega,$$

the transfer function $G(s)$ can be fitted to the measured frequency response data $G_M(\omega)$, and the parameters K, ω_0 and ξ can be determined. This process was executed for the three axes of the force sensor (with $\omega_1 = 10$ Hz and $\omega_2 = 400$ Hz) and the results are shown in Table 2. Figure 12 also shows three additional characteristics of the observed system's behavior:

1. Disturbances at 50 Hz caused by the alternating-current electric power supply
2. Coupling between the axes at resonance frequencies (at approx. 200, 220 and 280 Hz)
3. A frequency-dependent phase shift caused by the sensor amplifier

These characteristics are not considered by the transfer function $G(s)$.

Table 2: Results of the parametric identification

Axis	K	ω_0 (Hz)	ξ
X	0.1851	222.1	0.0142
Y	0.3137	199.6	0.0138
Z	0.1308	278.2	0.0071

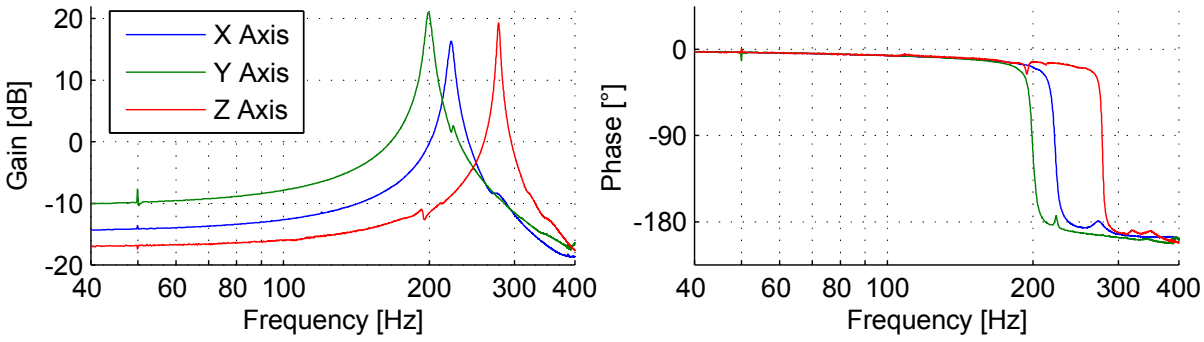

Figure 12: Frequency response for X, Y and Z axis

A comparison of the dc gain K determined in the parametric optimization with calibration coefficients evaluated using static calibration yields results within the boundaries of the measurement uncertainty evaluated in Table 1 while the y-axis has a deviation of 8,5 %.

5. CONCLUSION

In this paper, a calibration setup for dynamic forces by using a voice-coil actuator is described and contributions to static calibration uncertainty are estimated. The setup, which allows using different test-signals, is applied to the measurement of the frequency responses of every component of a three-component force sensor. The measurement results as well as the advantages and disadvantages of the test signals are discussed. From the frequency responses the parameters of a second-order transfer function model for every axis are identified. These values give a good approximation for the behavior of the main components of the sensor up to an operating frequency 400 Hz. The modeling allows the design of inverse filters which decrease the measurement error at operating frequencies close to the resonance frequency of the sensor. The measurement results shown in this paper contain the response of force sensor and of the measurement amplifier. Despite the small influence of the amplifier in the frequency range of interest, the results could be improved by deconvolution of the measurement results with the response of the amplifier, which was measured separately in 4.1.

ACKNOWLEDGEMENTS

The authors are grateful to the German Science Foundation (Deutsche Forschungs-gemeinschaft) for financial support of this work in the framework of the Research Training Group 'Lorentz force velocimetry and Lorentz force eddy current testing'.

REFERENCES

[1] Eichstädt, S.; Link, A.; Elster, C.: Dynamic Uncertainty for Compensated Second-Order Systems. Sensors 2010, 10, 7621-7631.
[2] Nishiwakit, K. et al.: A Six-axis Force Sensor with Parallel Support Mechanism to Measure the Ground Reaction Force of Humanoid Robot, IEEE International Conference on Robotics & Automation, 2002
[3] Heinicke, C. et al.: Interaction of a small permanent magnet with a liquid metal duct flow, J. Appl. Phys. 112, 124914, 2012
[4] Brauer H., Ziolkowski M., Eddy current testing of metallic sheets with defects using force measurements, Serbian Journal of Electrical Engineering, vol. 5, No. 1, 2008, pp. 11-20.
[5] Lorentz force eddy current testing: a prototype model, Journal of Nondestructive Evaluation, vol. 31, issue 4, 2012, pp. 357-372
[6] Uhlig R.P., Zec M., Ziolkowski M., Brauer H., Thess A., Lorentz force sigmometry: a contactless method for electrical conductivity measurements, Journal of Applied Physics, 111, 094914 (2012).
[7] Link, A. et al. System identification of force transducers for dynamic measurements, IMEKO World Congress, 2009
[8] Fujii, Y.; Fujimoto, H.: Proposal for an impulse response evaluation method for force transducers, Meas. Sci. Technol. 10 N31, 1999
[9] Park, Y.; Kumme, R.; Kang, D.: Dynamic investigation of a three-component force-moment sensor, Meas. Sci. Technol. 13, 2002
[10] Hilbrunner, F. et al.: Comparison of different load changers for EMFC-balances. - In: IMEKO TC3 & TC5 & TC22 International Conference / IMEKO TC3 International Conference; (Pattaya) : 2010.11.21-25. - Klong Luang, Pathumthani : (2010), pp. 65-68

[11] https://www.dspace.com/de/gmb/home/products/hw/modular_hardware_introduction/processor_boards/ds1006.cfm (30.07.2014)
[12] Wegfraß, A. et al.: Flow rate measurement of weakly conducting fluids using Lorentz force velocimetry. - In: Measurement science and technology. - Bristol: IOP Publ., Bd. 23, 2012, 10, 105307, 6 pages.
[13] http://www.me-systeme.de/de/datasheets/k3d40.pdf (26.05.2014)
[14] Isermann, R., Identifikation dynamischer Systeme 1: Grundlegende Methoden, Springer 1992, 2nd edition, 352 pages
[15] Lunze, J., Regelungstechnik 1: Systemtheoretische Grundlagen, Analyse und Entwurf Einschleifiger Regelungen, Springer 2013, 9th edition, 724 pages

CONTACTS

J. Schleichert, M.Sc. jan.schleichert@tu-ilmenau.de
M. Carlstedt, M.Sc. matthias.carlstedt@tu-ilmenau.de
R. Marangoni, M.Sc. rafael.marangoni@tu-ilmenau.de
Dr.-Ing. I. Rahneberg ilko.rahneberg@tu-ilmenau.de
Prof. Dr.-Ing. habil. T. Fröhlich thomas.fröhlich@tu-ilmenau.de